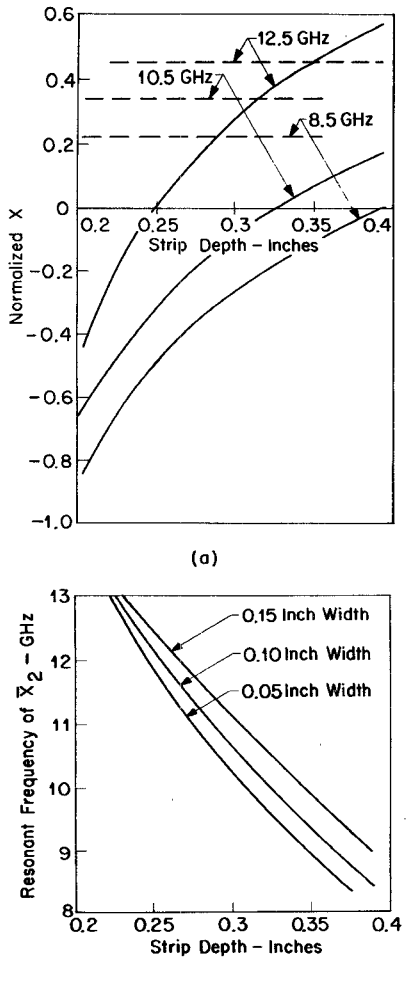

Fig. 7. The effect of insertion depth of a nontouching strip on the equivalent-circuit element values. (a) For a centered strip having $w = 0.15$ in; the solid line shows $\bar{X}_2$ and the broken line shows $\bar{X}_1$. (b) The resonant frequency of $\bar{X}_2$ as a function of depth for various values of w.

rectangular waveguide. The experimental values of input susceptance agree closely with the theoretical values. The resulting equivalent circuit has direct application in the design of microwave filters and tuning elements, and in the recently proposed planar circuits and fin-line structures.

References

[1] Y. Konishi, K. Uenakada, N. Yazawa, N. Hoshino, and T. Takahashi, "Simplified 12-GHz low-noise converter with mounted planar circuit in waveguide," *IEEE Trans. Microwave Theory Tech.*, vol. MTT-22, pp. 451–454, April 1974.

[2] Y. Konishi, K. Uenakada, and N. Hoshino, "The design of planar circuit mounted in waveguide and the application to low noise 12-GHz converter," *1974 IEEE S-MTT International Microwave Symposium Digest*, pp. 168–170.

[3] Y. Konishi and K. Uenakada, "The design of a bandpass filter with inductive strip—planar circuit mounted in waveguide," *IEEE Trans. Microwave Theory Tech.*, vol. MTT-22, pp. 869–873, October 1974.

[4] P. J. Meier, "Two new integrated-circuit media with special advantages at millimeter wavelengths," *1972 IEEE-GMTT International Microwave Symposium Digest*, pp. 221–223.

[5] ——, "Equivalent relative permittivity and unloaded Q factor of integrated finline," *Electronics Letters*, vol. 9, pp. 162–163, April 5, 1973.

[6] ——, "Integrated fin-line millimeter components," *1974 IEEE S-MTT International Microwave Symposium Digest*, pp. 195–197.

[7] ——, "Integrated fin-line millimeter components," *IEEE Trans. Microwave Theory Tech.*, vol. MTT-22, pp. 1209–1216, December 1974.

[8] K. Chang and P. J. Khan, "Analysis of a narrow capacitive strip in waveguide," *IEEE Trans. Microwave Theory Tech.*, vol. MTT-22, pp. 536–541, May 1974.

[9] L. Lewin, *Advanced Theory of Waveguides*. London, England: Iliffe, 1951.

On the Theory of Coupling Between Finite Dielectric Resonators

LARS PETTERSSON, STUDENT MEMBER, IEEE

***Abstract*—The coupling coefficients between open dielectric resonators in three useful dielectric-filter configurations, calculated from an electric rather than from a magnetic excitation of the fields, are given. The limitations of the latter method are pointed out and experimental results are given which supports the first method and shows that the differences cannot always be neglected.**

Introduction

Mutually coupled dielectric resonators in a waveguide under cutoff form a useful class of microwave bandpass filters [1], [2]. Since an exact field analysis of such a filter is a formidable problem, various approximate methods have been used. In order to calculate the resonance frequencies and internal fields of the resonators, one usually uses the so-called magnetic-wall model [3]. To calculate the coupling between two resonators or between a resonator and the waveguide fields various magnetic-dipole approximations have been used [1], [2], [4], [5]. In this short paper we will treat these coupling problems by calculating the excited waveguide fields directly from the polarization current density. This is also shown to be theoretically more correct than the magnetic-dipole methods. When we make the actual calculations we use the magnetic-wall model to obtain the polarization currents. We then get formulas which are almost as easy to use as the ones previously used. These formulas indicate that the commonly used magnetic-dipole approximations can give substantial errors in coupling strength. Experimental results obtained with two TiO_2-resonators, $\varepsilon_r = 90$, also support this method compared to the magnetic-dipole methods.

The Excitation Amplitude

Suppose that we in some way have found the fields inside the resonator and want to find the related waveguide fields for $z > A/2$, in Fig. 1. To do this we will use the polarization current $\bar{J}_p$ as current density $\bar{J}$ in the waveguide or, if $\varepsilon_{r2} \neq 1$, the excess polarization current density $j\omega\ \varepsilon_0(\varepsilon_{r1} - \varepsilon_{r2})\bar{E}$. In the following we will, however, assume that $\varepsilon_{r2} = 1$.

We expand the waveguide fields in orthogonal modes as

$$\bar{E}^{\pm} = \sum_n C_n^{\pm}(\bar{e}_n \pm \bar{e}_{zn})e^{\mp j\beta_n z} = \sum_n C_n^{\pm}\bar{E}_n^{\pm} \tag{1}$$

$$\bar{H}^{\pm} = \sum_n C_n^{\pm}(\pm \bar{h}_n + \bar{h}_{zn})e^{\mp j\beta_n z} = \sum_n C_n^{\pm}\bar{H}_n^{\pm} \tag{2}$$

and get [6]

$$C_n^{+} = -\frac{1}{P_n}\int_V \bar{J}_p \cdot \bar{E}_n^{-}\, dV \tag{3}$$

where

$$P_n = 2\int_{\substack{\text{waveguide}\\ \text{cross}\\ \text{section}}} \bar{e}_n \times \bar{h}_n \cdot \hat{z}\, ds. \tag{4}$$

So far we have not introduced any approximations. In the magnetic-wall model we may obtain expressions for the fields inside the resonator [3]. In this model the surfaces $y' = \pm B/2$ and $z' = \pm A/2$ in Fig. 1 are perfect magnetic conductors. It is

Manuscript received March 20, 1975; revised March 5, 1976.

The author is with the Research Laboratory of Electronics, Chalmers University of Technology, Gothenburg, Sweden.

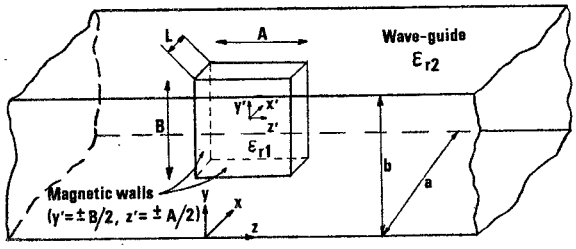

Fig. 1. A dielectric resonator transversely oriented in the center of a rectangular waveguide. $x' = x - a/2$; $y' = y - b/2$; $z' = z$.

valid with good accuracy for our purpose if ε_{r1} is large enough and if there are not metal walls close to the resonator.

The resonator fields in the magnetic-wall model are

$$H_{x'} = H_0 \cos\frac{\pi z'}{A} \cos\frac{\pi y'}{B} \cos\gamma_i x' \tag{5a}$$

$$H_{y'} = H_0 \frac{\gamma_i}{\pi B\left(\frac{1}{A^2}+\frac{1}{B^2}\right)} \cos\frac{\pi z'}{A} \sin\frac{\pi y'}{B} \sin\gamma_i x' \tag{5b}$$

$$H_{z'} = H_0 \frac{\gamma_i}{\pi A\left(\frac{1}{A^2}+\frac{1}{B^2}\right)} \sin\frac{\pi z'}{A} \cos\frac{\pi y'}{B} \sin\gamma_i x' \tag{5c}$$

$$E_{x'} = 0 \tag{5d}$$

$$E_{y'} = j\omega\mu_0 \frac{H_0}{A\pi\left(\frac{1}{A^2}+\frac{1}{B^2}\right)} \sin\frac{\pi z'}{A} \cos\frac{\pi y'}{B} \cos\gamma_i x' \tag{5e}$$

$$E_{z'} = -j\omega\mu_0 \frac{H_0}{B\pi\left(\frac{1}{A^2}+\frac{1}{B^2}\right)} \cos\frac{\pi z'}{A} \sin\frac{\pi y'}{B} \cos\gamma_i x'. \tag{5f}$$

Applying this to (1)–(3) we obtain the waveguide fields when the resonator is transversely oriented in the center of a homogeneous waveguide (see Fig. 1)

$$\bar{E} = j\frac{2\pi Z_0 M}{\lambda_0 ab} \cdot \sum_{\substack{m\,\text{odd}\\ n\,\text{even}}} \varepsilon_{n0}(-1)^{(m+n+1)/2} K_{mn} \left[-\sin\frac{m\pi x}{a}\cos\frac{n\pi y}{b}\,\hat{y} + \frac{\pi n}{\alpha_{mn} b}\sin\frac{m\pi x}{a}\sin\frac{n\pi y}{b}\,\hat{z}\right] e^{-\alpha_{mn} z} \tag{6a}$$

$$\bar{H} = \frac{M}{ab}\sum_{\substack{m\,\text{odd}\\ n\,\text{even}}} \varepsilon_{n0}(-1)^{(m+n+1)/2} K_{mn} \left[\frac{\alpha_{m0}^2}{\alpha_{mn}}\sin\frac{m\pi x}{a}\cos\frac{n\pi y}{b}\,\hat{x} + \frac{mn\pi^2}{ab\alpha_{mn}}\cos\frac{m\pi x}{a}\sin\frac{n\pi y}{b}\,\hat{y} + \frac{m\pi}{a}\cos\frac{m\pi x}{a}\cos\frac{n\pi y}{b}\,\hat{z}\right] e^{-\alpha_{mn} z} \tag{6b}$$

where

$$M = \frac{(\varepsilon_{r1}-1)H_0 ABL \cdot 16}{\lambda_0^2\pi^2\left(\frac{1}{A^2}+\frac{1}{B^2}\right)} \frac{\sin\gamma_i L/2}{\gamma_i L/2} \tag{7}$$

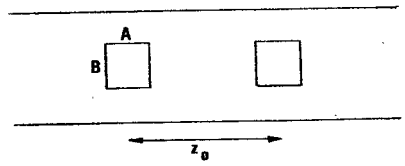

Fig. 2. Two coupled, transversely oriented, dielectric resonators.

is equal to the magnetic-dipole moment of the resonator, γ_i is the constant of propagation in the $\hat{x}'$ direction inside the resonator

$$\varepsilon_{n0} = \begin{cases} 1, & \text{if } n = 0 \\ 2, & \text{if } n \neq 0 \end{cases} \tag{8}$$

α_{mn} is the constant of attenuation in the waveguide for mode (m,n), and

$$K_{mn} = K_{mn}^{(y)} \cdot K_{mn}^{(z)} \cdot K_{mn}^{(x)} = \frac{\cos\frac{n\pi B}{2b}}{1-\left(\frac{nB}{b}\right)^2} \cdot \frac{\cosh\frac{\alpha_{mn}A}{2}}{1+\left(\frac{\alpha_{mn}A}{\pi}\right)^2} \cdot \frac{\left(\cos\frac{m\pi L}{2a} - \frac{m\pi}{a\gamma_i}\sin\frac{m\pi L}{2a}\cot\frac{\gamma_i L}{2}\right)}{1-\left(\frac{m\pi}{a\gamma_i}\right)^2} \tag{9}$$

is a correction factor which tells how much the amplitudes change when the resonator cannot be considered very small. Note that $K_{mn} \to 1$ when $B/b \to 0$, $\alpha_{mn}A \to 0$ and $1/a\gamma_i \to 0$ (that is $L/a \to 0$ since $\gamma_i L \approx$ constant).

In the formula for γ_i

$$\gamma_i = \sqrt{\left(\frac{2\pi f_0}{c_0}\right)^2 \varepsilon_{r1} - \pi^2\left(\frac{1}{A^2}+\frac{1}{B^2}\right)} \tag{10}$$

it is probably better to use the measured resonance frequency f_0 than the value obtained from the magnetic-wall model. Also, since the electric filling factor is much larger than the magnetic filling factor we will use the explicit expression for the electrical energy in all energy calculations, thus making the error as small as possible since the internal fields are better known than the external.

Two Coupled Resonators

We are now going to study the two-resonator system shown in Fig. 2. The magnetic coupling coefficient, to be used in an equivalent circuit, we calculate from the separation of the resonance frequencies f_1 and f_2, obtained when the fields are in and out of phase, respectively. From perturbation theory ([8], with the small modification of introducing ε_r in the derivation) we get

$$\omega - \omega_0 = \frac{j\int_V \bar{E}_0^* \cdot \bar{J}_p\, dV}{\int_V (\varepsilon_0\varepsilon_r \bar{E}_0^* \cdot \bar{E} + \mu_0 \bar{H}_0^* \cdot \bar{H})\, dV}$$

where $\bar{E}_0$ is the unperturbed field of one resonator, $\bar{J}_p$ is the polarization current density of the other, and $\bar{E}$ is the total perturbed field.

We now assume weak coupling so that the field distribution inside the resonators is unchanged and the correlation energy in the denominator is much less than the self-energy. Then we can use (5d)–(5f) to obtain $\bar{J}_p$, (6a) for $\bar{E}_0$ in the numerator, and put $\bar{E}$ equal to $\bar{E}_0$ and the magnetic energy equal to the electric

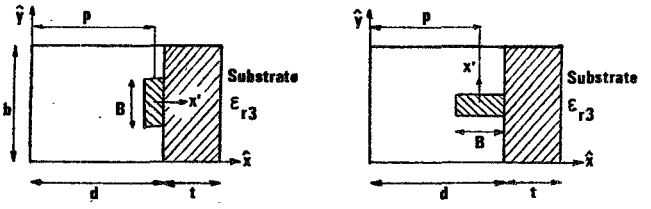

Fig. 3.

energy in the denominator. This gives

$$k = \frac{f_2 - f_1}{f_0} = -\frac{M^2\mu_0}{2W_1 ab} \sum_{\substack{m\ \text{odd} \\ n\ \text{even}}} \varepsilon_{n0} K_{mn}{}^2 \frac{\alpha_{m0}{}^2}{\alpha_{mn}} e^{-\alpha_{mn} z_0} \quad (11)$$

where z_0 is the center distance between the resonators and W_1 is the stored energy of one resonator [2, eq. (11)]. Hence we see that we obtain the same result as when the resonator is treated as a single magnetic dipole [1], except for the correction factors $K_{mn}{}^2$. (A slightly different definition of M is used in [1] which, however, does not affect the present comparison.)

If the resonator cannot be considered very small or if we want to find the fields close to the resonators so that higher modes must be taken into account, the correction factors K_{mn} in (6) and (11) cannot always be neglected.

Two other interesting cases are when the resonators are placed on a substrate as shown in Fig. 3(a) and (b). The natural modes in these cases are LSE- and LSM-modes [7]. In the case of Fig. 3(b), (5a)–(5e) are still valid, while in the case of Fig. 3(a) we have to replace the argument $\gamma_i x'$ by $\gamma_i x' + \phi_{x'}$ since we no longer have a symmetry in the x' direction [2]. In the practical cases of interest, however, $\phi_{x'}$ is quite small. We also introduce the variables h_m and l_m, being the constants of propagation in the $\hat{x}$ direction in the air and substrate regions, respectively, and the factors

$$D_{mE} = d - \frac{\sin 2h_m d}{2h_m} + \frac{\sin^2 h_m d}{\sin^2 l_m t}\left(t - \frac{\sin 2l_m t}{2l_m}\right) \quad (12a)$$

$$D_{mH} = d + \frac{\sin 2h_m d}{2h_m} + \frac{\cos^2 h_m d}{\varepsilon_{r3} \cos^2 l_m t}\left(t + \frac{\sin 2l_m t}{2l_m}\right) \quad (12b)$$

but keep the definitions for M and W_1.

In the case of Fig. 3(a) we obtain

$$k = -\frac{M^2\mu_0}{2W_1 b} \sum_{\substack{n\ \text{even} \\ \text{LSE}}} \varepsilon_{n0} \frac{K_{mn}'{}^2 \alpha_{m0}{}^2 e^{-\alpha_{mn} z_0}}{\alpha_{mn} D_{mE}} \quad (13)$$

where we obtain K_{mn}' from (9) by changing $K_{mn}{}^{(x)}$ to

$$\frac{1}{2 \sin \gamma_i L/2}\left\{\frac{\sin (h_m + \gamma_i)L/2 \cdot \sin (h_m p + \phi_{x'})}{h_m/\gamma_i + 1} + \frac{\sin (h_m - \gamma_i)L/2 \cdot \sin (h_m p - \phi_{x'})}{h_m/\gamma_i - 1}\right\}.$$

In the case of Fig. 3(b) we obtain

$$k = -\frac{M^2\mu_0}{W_1 b}\left\{\sum_{\substack{n\ \text{odd} \\ \text{LSE}}} \frac{h_m{}^2 K_{mn}''{}^2 \left(\frac{n\pi}{b}\right)^2 e^{-\alpha_{mn} z_0}}{\alpha_{m0}{}^2 \alpha_{mn} D_{mE}} - \frac{4\pi^2}{\lambda_0{}^2} \sum_{\substack{n\ \text{odd} \\ \text{LSM}}} \frac{\alpha_{mn} K_{mn}''{}^2 e^{-\alpha_{mn} z_0}}{\alpha_{m0}{}^2 D_{mH}}\right\} \quad (14)$$

where all variables in the first sum are calculated for LSE-modes and in the second for LSM-modes and where we obtain K_{mn}'' from (9) by multiplying by $\cos h_m p$ and replacing $n\pi/b$ by h_m and $m\pi/a$ by $n\pi/b$.

Discussion of Other Methods

Various authors [1], [2], [4], [5] have, instead of using the polarization current, used a magnetization as the source of the waveguide fields. We are now going to show that this leads to theoretical problems and that such approximations give errors that cannot always be neglected. To do this we will try to identify $\bar{J}_p$ in (3) with a magnetization $\bar{M}$ and a potential Q according to

$$\nabla \times \bar{H} = \bar{J}_p + j\omega\varepsilon_0 \bar{E} = \nabla \times \bar{M} + \nabla Q + j\omega\varepsilon_0 \bar{E}. \quad (15)$$

If we define $\bar{H}' = \bar{H} - \bar{M}$ we get

$$\nabla \times \bar{H}' = \nabla Q + j\omega\varepsilon_0 \bar{E} \quad (16)$$

$$\nabla \times \bar{E} = -j\omega\bar{B} = -j\omega\mu_0 \bar{H}' - j\omega\mu_0 \bar{M} \quad (17)$$

where we are free to set $\nabla \cdot \bar{M} = 0$.

Hence we get a magnetic current $j\omega\mu_0\bar{M}$, and if $\bar{M}$ and ∇Q equals zero for $z > A/2$, we get for the excitation amplitude in analogy with (3)

$$C_n^+ = \frac{j\omega\mu_0}{P_n} \int \bar{H}_n^- \cdot \bar{M}\, dV - \frac{1}{P_n} \int \nabla Q \cdot \bar{E}_n^-\, dV. \quad (18a)$$

Now we want to represent the resonator with a magnetization only; that is, we want to put $\nabla Q = 0$, and

$$C_n^+ = \frac{j\omega\mu_0}{P_n} \int \bar{H}_n^- \cdot \bar{M}\, dV. \quad (18b)$$

However, since $\rho = 0$, we have

$$\nabla^2 Q = j\omega \nabla \cdot \bar{P} = -j\omega \bar{D} \cdot \nabla \frac{1}{\varepsilon_r} \quad (19)$$

which equals zero only if either ε_r = constant, which is not the case here, or if $\bar{D} \perp \nabla(1/\varepsilon_r)$. Consequently, if ε_r is constant inside the resonator, the requirement $\nabla^2 Q = 0$ is satisfied only if $\bar{D}$ is parallel to the resonator surface. This is true in the magnetic-wall model but not in a more realistic case. We conclude therefore that it is not, in general, possible to obtain an exact solution using only the magnetization.

Let us now look at the idealized case for which $\bar{D} \perp \nabla(1/\varepsilon_r)$. According to [1], a reasonable assumption is that $\bar{M}$ averaged along the resonator axis is proportional to $\bar{B}$, that is $\bar{M} \sim \bar{H}$, and according to [2] we should use $\bar{M} \sim \varepsilon_r \bar{H}$. However, for $\bar{M}$ to be proportional to $\bar{H}$ inside the resonator we must have

$$\bar{M} = \left(1 - \frac{1}{\varepsilon_r}\right) \bar{H} \quad (20)$$

because only then

$$\nabla \times \bar{M} = j\omega(\varepsilon_r - 1)\varepsilon_0 \bar{E} \quad (21)$$

is satisfied. On the surface of the resonator we then get

$$\nabla \times \bar{M} = \left(1 - \frac{1}{\varepsilon_r}\right) \nabla \times \bar{H} - \nabla\left(\frac{1}{\varepsilon_r}\right) \times \bar{H} = \bar{J}_p - \nabla\left(\frac{1}{\varepsilon_r}\right) \times \bar{H}. \quad (22)$$

The last term is equivalent to the surface current density

$$\bar{J}_{ms} = \hat{n} \times \delta\bar{M} = \left(\frac{1}{\varepsilon_{r1}} - 1\right) \hat{n} \times \bar{H} \tag{23}$$

which must exist for the magnetization to be discontinuous. Hence, the assumption that $\bar{M} \sim \bar{H}$ is, in general, incorrect. Note that in the magnetic-wall model this term is zero on the magnetic walls but not on the other walls. Note also that if the assumption that $\bar{M} \sim \bar{H}$ were correct the resonator would be equivalent to a magnetic resonator. We also see that $\bar{J}_{ms}$ is approaching the finite function $-\hat{n} \times \bar{H}$ as $\varepsilon_{r1} \to \infty$.

In fact, with (18b) together with (20) we get a correction factor K_{mn}''' for the case in Fig. 1 which is obtained from (9) by multiplying $\cos(m\pi L/2a)$ in $K_{mn}^{(x)}$ by

$$1 + \frac{\lambda_0^2}{4\varepsilon_{r1}}\left(\frac{m^2}{a^2} - \frac{\gamma_i^2}{\pi^2}\right).$$

This expression does not approach unity even when $\varepsilon_{r1} \to \infty$ unless $\gamma_i L \to 0$ at the same time.

We can also write Maxwell's equations in the form

$$\nabla \times \bar{D} = -j\omega\varepsilon_0\bar{B} + \nabla \times \bar{P} \tag{24a}$$

$$\nabla \times \bar{H} = j\omega\bar{D}. \tag{24b}$$

From this we obtain, in analogy with (18a), since $\varepsilon_{r2} = 1$

$$\begin{aligned} C_n^+ &= -\frac{1}{\varepsilon_0 P_n}\int_V \bar{H}_n^- \cdot \nabla \times \bar{P}\, dV \\ &= \frac{j\omega\mu_0}{P_n}\int_V (\varepsilon_{r1} - 1)\bar{H}_n^- \cdot \bar{H}\, dV \\ &\quad + \frac{1}{P_n}\int_{\substack{\text{resonator}\\ \text{surface}}} (\varepsilon_{r1} - 1)\bar{E} \times \bar{H}_n^-\, d\bar{S}. \end{aligned} \tag{25}$$

The first term in (25) seems to support the assumption made in [2] that $\bar{M} \sim \varepsilon_r\bar{H}$ for $\varepsilon_{r1} \to \infty$. In this case we can, however, definitely not neglect the second term, since the electric field has a maximum on the magnetic walls. In fact, the two terms in (25) must be of almost the same magnitude since the first term gives a value ε_{r1} larger than that obtained from (18b) together with (20) which, in turn, usually gives a much smaller error.

A third commonly used expression [4], [5] is to regard

$$\bar{M} = \tfrac{1}{2}\bar{r} \times \bar{J} \tag{26}$$

where $\bar{r}$ has its origin in the center of the resonator, as a distributed magnetization density. This is associated to the formula for the total dipole moment from a closed current loop

$$\bar{M}_{\text{tot}} = \frac{1}{2}\int \bar{r} \times \bar{J}\, dV. \tag{27}$$

However, (26) is in general not valid for large current loops. Applying (26) together with (18b) to the case in Fig. 1 we get a rather complicated expression for the correction factors $K_{mn}^{(x)}$, which, however, gives the correct result for small resonators.

The conclusion of this section is that (3) and (18b) with $\bar{M} \approx \bar{H}$ are not identical even if $\bar{D} \perp \nabla(1/\varepsilon_r)$ and $\varepsilon_{r1} \to \infty$, although the differences in the results are usually small. If the resonator can be considered very small, however, the approximation $\bar{M} = \tfrac{1}{2}\bar{r} \times \bar{J}$ can be used. In fact, it seems impossible to find a simple definition for $\bar{M}$ which fulfills the boundary conditions.

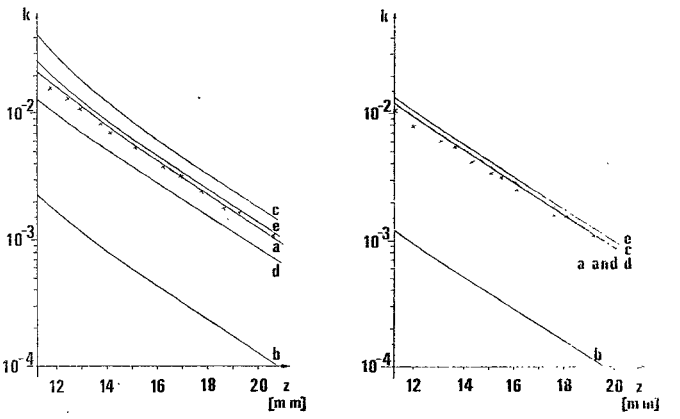

(a)

A = 10.16 mm
B = 5.08 mm
L = 1.51 mm
a = 10.16 mm
b = 22.86 mm
ε_{r1} = 90
f_0 = 6.345 GHz

x = experimental points
a) = theory (3)
b) = theory (18b) and (20)
c) = theory (18b) and (26)
d) = (11) with $K_{mn} = 1$
e) = b) normalized to = d), when $\varepsilon_{r1} \to \infty$

(b)

A = 5.08 mm
B = 10.16 mm
L = 1.51 mm
a = 10.16 mm
b = 22.86 mm
ε_{r1} = 90
f_0 = 6.345 GHz

Fig. 4.

Experimental Results

Two experiments have been made with resonators made of TiO_2, $\varepsilon_{r1} = 90$. The resonator dimensions were, in experiment I, $A = 10.16$ mm, $B = 5.08$ mm, and $L = 1.51$ mm; while in experiment II, A and B were interchanged. The resonators were placed in a waveguide with dimensions $a = 10.16$ mm and $b = 22.86$ mm, and the resonance frequencies were in both experiments 6.345 GHz. In Fig. 4(a) and (b) the measured coupling coefficients in experiments I and II are shown together with some theoretical curves, in which the magnetic-wall-model fields (5) have been used. Curve e) in Fig. 4 has been obtained by dividing the values in curve b) by a factor of $1 - (\lambda_0^2\gamma_i^2)/(4\varepsilon_{r1}\pi^2)$, which makes it equal to curve d) as $\varepsilon_{r1} \to \infty$.

From Fig. 4 we see that the experimental points are in good agreement with curve a) and that in Fig. 4(a) they are well separated from the usually used curve d) and also from curves b) and c). This result also supports the assumption that the magnetic-model fields are good approximations to the real fields for this purpose.

Conclusion

The coupling between dielectric resonators have been treated by starting from the polarization current density instead of the usually used magnetic-dipole moment. We thus obtained expressions which showed that the differences between the methods may be significant. Experiments have also been done which support the assumption that the method treated here gives quite accurate results also when we use a polarization current density obtained from the magnetic-wall model.

Acknowledgment

The author wishes to thank Dr. O. Nilsson and Dr. E. Kollberg for making many valuable suggestions about the manuscript.

References

[1] S. B. Cohn, "Microwave bandpass filters containing high-Q dielectric resonators," *IEEE Trans. Microwave Theory and Techniques*, vol. MTT-16, pp. 218–227, April 1968.

[2] T. D. Iveland, "Dielectric resonator filters for application in microwave integrated circuits," *IEEE Trans. Microwave Theory and Techniques*, vol. MTT-19, pp. 643–652, July 1971.

[3] A. Okaya and L. F. Barash, "The dielectric microwave resonator," *Proc. IRE*, vol. 50, pp. 2081–2092, Oct. 1962.
[4] J. L. Pellegrin, "The filling factor of shielded dielectric resonators," *IEEE Trans. Microwave Theory and Techniques*, vol. MTT-17, pp. 764–768, Oct. 1969.
[5] L. V. Alekseychik, V. M. Gevorkyan, and Yu A. Kazantzev, "Excitation of an open dielectric resonator in a transmission line," *Radiotekhnika i Elektronika*, vol. 17, pp. 1814–1821, Nov. 1972.
[6] R. E. Collin, *Foundations for Microwave Engineering*. New York: McGraw-Hill, 1966, pp. 183–190.
[7] ——, *Field Theory of Guided Waves*. New York: McGraw-Hill, 1960, pp. 224–232.
[8] R. F. Sohoo, *Theory and Applications of Ferrites*. Englewood Cliffs, NJ: Prentice-Hall, 1960, pp. 260–262.

Effect of Diode Parameters on Reflection-Type Phase Shifters

PRADEEP WAHI, STUDENT MEMBER, IEEE, AND K. C. GUPTA

***Abstract*—This short paper describes effects of series inductance, shunt capacitance, and resistances associated with p-i-n diodes on the performance of reflection-type digital phase shifters using a shorted transmission line behind a shunt-mounted diode. It is found that the shunt capacitance is the most dominant reactance influencing the phase shift and it increases the phase-shift value. The series inductance reduces the phase-shift value. Expressions for phase shift in various cases are presented.**

Introduction

One of the design configurations for a reflection-type phase shifter consists of a p-i-n diode shunt mounted across a transmission line at a distance l from the shorted end [1]. Phase of the reflected wave at the diode plane changes when the bias on the diode is changed from forward to reverse, as the later implies inclusion of an additional line length l. Thus the phase shift obtained is given approximately by $2\beta l$ where β is the phase constant of the line. This arrangement is converted into a two-port phase shifter by using a circulator or a hybrid.

A simple procedure for designing such a phase shifter assumes the p-i-n diode to be ideal, i.e., short circuit when forward biased and open circuit when reverse biased. This method does not yield accurate result at higher frequencies when parasitic reactances and resistances associated with the diode become significant. This short paper describes the effect of diode reactances and resistances on the phase-shift characteristics of this type of phase shifter.

Diode Parameters

The important parameters of a p-i-n diode are; series inductance L (typically 0.4–2.0 nH), shunt capacitance C (0.1–2 pF), forward-bias series resistance R_s (0.5–2.0 Ω), and reverse-bias shunt resistance R ($\simeq$ 10 kΩ). The effect of these parameters may be considered analytically by taking them one by one in association with an ideal switch. Phase-shift and insertion-loss calculations are carried out by adding the diode admittance to the admittance of the line behind the diode and finding out the refiection coefficient caused by this combination.

Effect of Series Inductance

When an inductance L is in series with the ideal switch (Fig. 1 inset) the phase-shift expression is obtained as

$$\phi = 2\beta l + 2\tan^{-1}\left[\cot \beta l + Z_0/\omega L\right] - \pi. \tag{1}$$

Manuscript received February 3, 1975; revised January 26, 1976.
The authors are with the Advanced Centre for Electronic Systems, IIT, Kanpur, India.

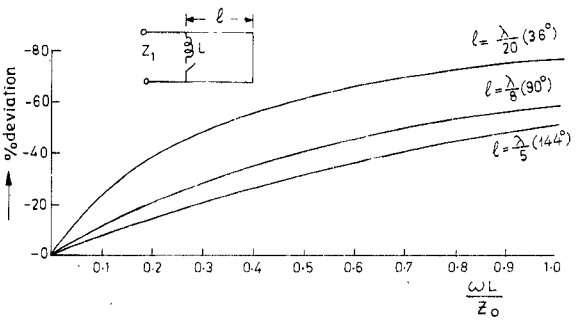

Fig. 1. Effect of series inductance L on the phase shift.

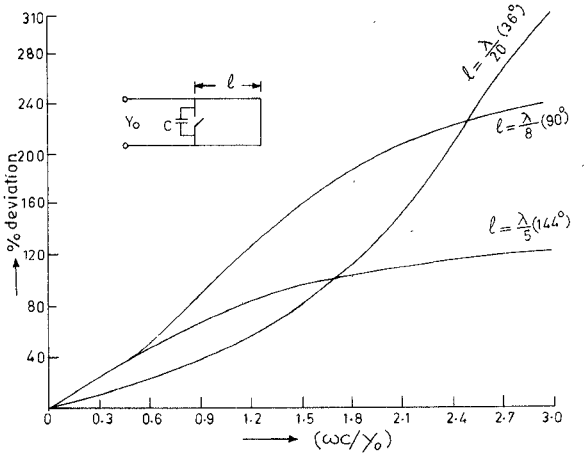

Fig. 2. Effect of shunt capacitance C on the phase shift.

It may be noted that the phase shift ϕ varies with both the line length behind the diode and the reciprocal of the normalized reactance ($Z_0/\omega L$). Differentiating (1) with respect to L one gets

$$\frac{\partial \phi}{\partial L} = \frac{2}{\left[1 + \left(\cot \beta l + \frac{Z_0}{\omega L}\right)^2\right]} \frac{Z_0}{\omega}\left(-\frac{1}{L^2}\right) \tag{2}$$

which shows that the phase shift decreases with an increase in L. The percentage deviation of the phase shift from an ideal case versus the normalized series reactance is plotted for three different cases in Fig. 1. It is seen that the deviation from the ideal case increases with the value of L. Also the deviation is higher for smaller values of phase shift (βl).

Effect of Shunt Capacitance

The expression for phase shift for the case when there is a capacitance in parallel with ideal switch (Fig. 2) is found to be

$$\phi = 2\tan^{-1}\left[\frac{\omega c}{Y_0} - \cot \beta l\right] - \pi. \tag{3}$$

The phase shift varies with both the length and the normalized shunt susceptance. Differentiating (3) with respect to capacitance C

$$\frac{\partial \phi}{\partial C} = \frac{1}{\left[1 + \left(\frac{\omega C}{Y_0} - \cot \beta l\right)^2\right]}\left(\frac{\omega}{Y_0}\right) \tag{4}$$

which is always positive. Hence the phase shift always increases with an increase in the capacitance value. The effect of increase